

# On the Performance of Network NOMA in Uplink CoMP Systems: A Stochastic Geometry Approach

Yanshi Sun, Zhiguo Ding, *Senior Member, IEEE*, Xuchu Dai, and Octavia A. Dobre, *Senior Member, IEEE*

## Abstract

To improve the system throughput, this paper proposes a network non-orthogonal multiple access (N-NOMA) technique for the uplink coordinated multi-point transmission (CoMP). In the considered scenario, multiple base stations collaborate with each other to serve a single user, referred to as the CoMP user, which is the same as for conventional CoMP. However, unlike conventional CoMP, each base station in N-NOMA opportunistically serves an extra user, referred to as the NOMA user, while serving the CoMP user at the same bandwidth. The CoMP user is typically located far from the base stations, whereas users close to the base stations are scheduled as NOMA users. Hence, the channel conditions of the two kind of users are very distinctive, which facilitates the implementation of NOMA. Compared to the conventional orthogonal multiple access based CoMP scheme, where multiple base stations serve a single CoMP user only, the proposed N-NOMA scheme can support larger connectivity by serving the extra NOMA users, and improve the spectral efficiency by avoiding the CoMP user solely occupying the spectrum. A stochastic geometry approach is applied to model the considered N-NOMA scenario as a Poisson cluster process, based on which closed-form analytical expressions for outage probabilities and ergodic rates are obtained. Numerical results are presented to show the accuracy of the analytical results and also demonstrate the superior performance of the proposed N-NOMA scheme.

Y. Sun and X. Dai are with the Key Laboratory of Wireless-Optical Communications, Chinese Academy of Sciences, School of Information Science and Technology, University of Science and Technology of China, No. 96 Jinzhai Road, Hefei, Anhui Province, 230026, P. R. China. (email: sys@mail.ustc.edu.cn, daixc@ustc.edu.cn).

Z. Ding is with the School of Electrical and Electronic Engineering, the University of Manchester, Manchester M13 9PL, U.K. (email:zhiguo.ding@manchester.ac.uk).

O. A. Dobre is with the Faculty of Engineering and Applied Science, Memorial University, St. Johns, NL A1B 3X5, Canada (e-mail: odobre@mun.ca)).

## Index Terms

network NOMA (N-NOMA), coordinated multi-point (CoMP), stochastic geometry (SG), Poisson cluster process (PCP), multiple access.

## I. INTRODUCTION

Recently, non-orthogonal multiple access (NOMA) has attracted significant research attentions in both academia and industry community, not only due to its superior spectral efficiency but also because of its compatibility with other advanced communication techniques [1]–[4]. The key idea of NOMA is to serve more than one user in each orthogonal channel resource block, e.g., a time slot, a frequency channel, a spreading code, or an orthogonal spatial degree of freedom. NOMA has been recognized as a key enabling multiple access technique for the fifth generation (5G) mobile networks. For example, downlink NOMA has been adopted by 3GPP-LTE systems as multiuser superposition transmission (MUST) [5]. Moreover, NOMA has been recently proposed for the forthcoming digital TV standard (ATSC 3.0), where it is referred to as layered division multiplexing (LDM) [6].

### *A. Related Literature*

The concept of NOMA was initially proposed in [1] for future wireless networks. The performance of NOMA with randomly deployed users in a downlink scenario was investigated in [7], which shows that NOMA can outperform conventional orthogonal multiple access (OMA) in terms of outage performance and ergodic sum rates. To enhance the performance of users with weak channel conditions, cooperative NOMA was proposed in [8] by treating users with strong channel condition as relays. The user fairness of NOMA was studied in [9], and in [10], the authors characterized the impact of user pairing on the performance of two types of NOMA systems, i.e., NOMA with fixed power allocation (F-NOMA) and cognitive-radio-inspired NOMA (CR-NOMA). In [11]–[13], resource allocation for NOMA was investigated. In [14] and [15], the authors studied the performance of uplink NOMA by considering inter-cell interference.

Note that, [7]–[12], [14], [15] focus on single-carrier NOMA, where the principle of NOMA is implemented on a single resource block. Besides single-carrier NOMA, there are also NOMA schemes termed multi-carrier NOMA, where the principle of NOMA is implemented on multiple resource blocks, e.g., sparse code multiple access (SCMA) [16] and pattern-division multiple

access (PDMA) [17]. Different from single-carrier NOMA which mainly exploits power-domain for multiplexing, multi-carrier NOMA can exploit code-domain across multiple resource blocks to further improve system performance.

Furthermore, it has been shown that NOMA can be combined with many other advanced communication techniques. For example, the application of NOMA in millimeter-wave (mmWave) communications was investigated in [18], [19]. The combination of NOMA and multiple-input multiple-output (MIMO) techniques was studied in [20]–[23]. Moreover, NOMA was also applied to relay systems [24], as well as to wireless caching [25].

### *B. Motivations and Contributions*

Coordinated multipoint (CoMP) has been recognized as an important enhancement for LTE-A [26]–[28]. CoMP was mainly proposed to improve cell-edge users' data rates and hence improve the cell coverage. Conventional CoMP schemes [29], [30] in the literature are based on OMA, where multiple base stations cooperatively serve a single user. A drawback of these OMA based schemes is that, once a channel resource block is occupied by a cell-edge user, it cannot be accessed by other users. Thus, the spectral efficiency becomes worse as the number of cell-edge users increases. Note that, the channel connection of a cell-edge user to a base station can be much worse than that of a user close to the corresponding base station, due to large scale path loss. Inspired by this observation, network NOMA (N-NOMA) schemes were proposed in the downlink CoMP systems [31], [32]. The key idea of N-NOMA is to schedule additional users close to the base stations, and allow cell-edge users and near users to be served simultaneously at the same channel resource block, by combining CoMP which harvests spatial degrees of freedom with NOMA which improves the spectral efficiency. More specifically, in [31], the Alamouti code was applied to improve the cell-edge user's reception reliability, while in [32], distributed analog beamforming was applied.

The aforementioned N-NOMA schemes in [31] and [32] mainly focus on the downlink scenario and particular network topologies, e.g., one-dimensional topology is considered in [31] and equilateral triangle topology in [32]. Different from [31] and [32], this paper studies the application of N-NOMA in the uplink CoMP scenario in a general network topology. Particularly, a cell-edge user (termed the CoMP user) is set at the origin, the base stations and their associated near users form a Poisson Cluster process (PCP) [33], [34], where the base stations are treated as parents, and their associated near users are offsprings. Each base station chooses a user

from its offsprings, which is referred to as a NOMA user. The CoMP user and the NOMA users simultaneously transmit messages to the base stations. After receiving the superimposed messages, each base station applies successive interference cancellation (SIC) to first decode its NOMA user's message. If successful, it can remove the NOMA user's message and then deliver the remaining message as well as the decoded NOMA user's message to the network controller, which is connected with all the base stations through wired links. Finally, the CoMP user's message is decoded at the network controller. The contributions of this paper are listed in the following:

- The performance of the NOMA users is first investigated. The probability density function (pdf) of the composite channel gain which consists of Rayleigh fading and large scale path loss is first obtained and approximated by applying the Gaussian-Chebyshev approximation. Decoding the NOMA user's message suffers from two kinds of interferences, the interference from the CoMP user and the inter-cell interferences. The Laplace transforms for both kinds of interferences are then applied to facilitate the analysis. Closed-form expressions for the outage probabilities and ergodic rates achieved by the NOMA users are then obtained.
- The study of the CoMP user's performance is divided into two cases.
  - In the first case, inspired by cognitive radio (CR), the NOMA users' data rates are adaptively adjusted according to their instantaneous channel conditions, in order to not degrade the CoMP user's performance compared to OMA based uplink CoMP.
  - In the second case, the NOMA users' data rates are fixed. Note that, only the base stations which can successfully remove their NOMA users' messages are allowed to participate in CoMP, which thins the initial point process. However, in a realization of the point process, the thinning probabilities of different nodes are correlated, since they interfere with each other. Besides, the thinning probability changes over different realizations of the point process, since the topology is different in different realizations of the point process. The above two facts make the analysis for the outage probability of the CoMP user challenging. To get insight into this case, we turn to study a simplified scheme, namely the nearest N-NOMA scheme. In the nearest N-NOMA scheme, only one base station, which is nearest to the CoMP user, is invited to apply NOMA to serve the CoMP user and its NOMA user simultaneously. Closed-form expressions are obtained for outage probabilities achieved by the nearest N-NOMA scheme.

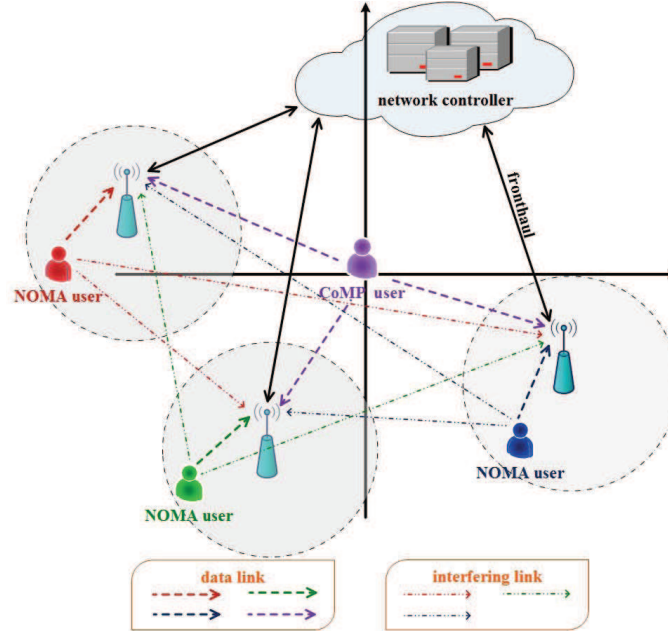


Fig. 1: An illustration of the system model.

- All the analytical results are validated by computer simulations. The comparison between the proposed N-NOMA scheme and OMA is illustrated, and it is concluded that the proposed N-NOMA scheme significantly improves the spectral efficiency compared to OMA.

### C. Organization

The rest of this paper is organized as follows. Section II illustrates the system model. Section III analyzes the performance of the proposed N-NOMA scheme. Section IV provides numerical results to demonstrate the performance of the proposed N-NOMA scheme and also verify the accuracy of the developed analytical results. Section V concludes the paper. Finally, Appendixes collect the proofs of the obtained analytical results.

## II. SYSTEM MODEL

### A. System Model

Consider an N-NOMA communication scenario as explained in the following. As illustrated in Fig. 1, there are multiple base stations which collaborate with each other to help a single CoMP user, denoted by  $U_0$ , which is similar to conventional CoMP. In addition, each base station will

opportunistically serve one extra user at the same time and frequency channel allocated to  $U_0$ . The extra user served by each base station is referred to as a NOMA user in this paper.

Without loss of generality, the CoMP user is placed at the origin. The locations of the base stations and the NOMA users are modeled as a PCP. In particular, assume that the locations of the base stations are denoted by  $x_i$  and modeled as a homogeneous Poisson point process (HPPP), denoted by  $\Phi_c$ , with density  $\lambda_c$ , i.e.,  $x_i \in \Phi_c$ . Each base station is the parent node of a cluster covering a disk whose radius is denoted by  $\mathcal{R}_c$ . To implement NOMA transmission, the base station in cluster  $i$ , denoted by  $BS_i$ , invites  $K$  users, denoted by  $U_{i,k}$ ,  $k \in \{1, \dots, K\}$ , to participate in NOMA transmission. These users associated with the same base station are viewed as offspring nodes. The locations of these users, denoted by  $y_{i,k}$ ,  $k \in \{1, \dots, K\}$ , are uniformly distributed in the disk with  $BS_i$  located at its origin. To simplify the notation, the locations of the cluster users are conditioned on the locations of their cluster heads. As such, the distance from a cluster user to its cluster head is  $\|y_{i,k}\|$ , and the distance from  $U_{i,k}$  to  $BS_j$  is  $\|y_{i,k} + x_i - x_j\|$ .

Among  $K$  users associated with  $BS_i$ ,  $U_{i,k_i^*}$  is selected for N-NOMA transmission, and the user selection criterion is to select the user with the largest composite channel gain as follows:

$$k_i^* = \arg \max_{k \in \{1, \dots, K\}} \frac{|h_{BS_i, U_{i,k}}|^2}{L(\|y_{i,k}\|)}. \quad (1)$$

where  $h_{BS_i, U_{j,k}}$  denotes the Rayleigh fading channel coefficient between  $BS_i$  and  $U_{j,k}$ , and  $L(\|y_{j,k}\|)$  denotes the path loss. Particularly, the following path loss model is used,  $\frac{\eta}{L(\|y_{j,k}\|)}$ , where  $L(\|y_{j,k}\|) = \|y_{j,k}\|^\alpha$ ,  $\eta = \frac{c^2}{16\pi^2 f_c^2}$  denotes the parameter relevant to carrier frequency  $f_c$  ( $c$  is light speed), and  $\alpha$  denotes the path loss exponent. It is worth pointing out that, throughout the paper, all base stations use the same user selection criterion as shown in (1).

In this paper, it is assumed that all nodes are equipped with a single antenna. This assumption is applicable in many scenarios in forthcoming 5G networks. For example, in applications that combine Internet-of-things (IoT) with cellular networks, randomly deployed low-cost IoT access points are more likely to have a single antenna.

It is also worth pointing out that, in this paper, the distance between the CoMP user and a base station is typically much larger than the distance of a NOMA user. Under this circumstance, the channel conditions will be distinctive enough to facilitate the implementation of NOMA.

## B. Description of N-NOMA

For uplink N-NOMA, the CoMP user, denoted by  $U_0$ , transmits its signal to all the base stations. In addition, the user with the largest composite channel gain in cluster  $i$  is invited to send its information to  $BS_i$ . Therefore,  $BS_i$  receives the following:

$$y_{BS_i} = \underbrace{\frac{\sqrt{\eta P_0} h_{BS_i, U_0}}{\sqrt{L} (\|x_i\|)}}_{\text{CoMP user's signal}} s_0 + \underbrace{\frac{\sqrt{\eta P} h_{BS_i, U_{i, k_i^*}}}{\sqrt{L} (\|y_{i, k_i^*}\|)}}_{\text{NOMA user's signal}} s_{i, k_i^*} + \underbrace{\sum_{x_j \in \Phi_c \setminus x_i} \frac{\sqrt{\eta P} h_{BS_i, U_{j, k_j^*}}}{\sqrt{L} (\|y_{j, k_j^*} + x_j - x_i\|)}}_{\text{Inter-cell interference}} s_{j, k_j^*} + n_i, \quad (2)$$

where  $P_0$  denotes the transmission power of the CoMP user,  $P$  denotes the NOMA users' transmission power,  $s_{i, k_i^*}$  denotes the message sent by  $U_{i, k_i^*}$ ,  $s_0$  is the message sent by  $U_0$ ,  $h_{BS_i, U_0}$  is defined similarly to  $h_{BS_i, U_{i, k}}$ , and  $n_i$  denotes the additive noise, which is modeled as a circular symmetric complex Gaussian random variable, i.e.,  $n_i \sim \mathcal{CN}(0, \sigma^2)$ , where  $\sigma^2$  is the noise power.

Among the three types of information in (2),  $BS_i$  will first decode its NOMA user's information, since this user in cluster  $i$  is very likely to be much closer to  $BS_i$  compared to the CoMP user. If successfully,  $BS_i$  will then subtract the NOMA user's signal from its observation, and pass the remaining signal as well as the decoded NOMA user's message to the network controller. Finally, the CoMP user's message is decoded at the network controller. The corresponding signal-to-interference-plus-noises (SINRs) for decoding these signals are provided in the following.

1) *Decoding the NOMA user's signal:* As discussed before, the NOMA users' signals are decoded first, by treating the CoMP user's signals as interference. In cluster  $i$ ,  $BS_i$  decodes its NOMA user's information with the following SINR ratio:

$$\text{SINR}_{k_i^*}^{BS_i} = \frac{\frac{|h_{BS_i, U_{i, k_i^*}}|^2}{L (\|y_{i, k_i^*}\|)}}{I_{\text{CoMP}}^U + I_{\text{inter}}^U + \frac{1}{\rho}}, \quad (3)$$

where  $\rho = \frac{\eta P}{\sigma^2}$ ,  $I_{\text{CoMP}}^U = \frac{\phi |h_{\text{BS}_i, \text{U}_0}|^2}{L(\|x_i\|)}$  denotes the interference from the CoMP user with  $\phi = \frac{P_0}{P}$ , and the inter-cluster interference is given by

$$I_{\text{inter}}^U = \sum_{x_j \in \Phi_c \setminus x_i} \frac{|h_{\text{BS}_i, \text{U}_{j, k_j^*}}|^2}{L(\|y_{j, k_j^*} + x_j - x_i\|)}. \quad (4)$$

The corresponding achievable data rate of  $\text{U}_{i, k_i^*}$  is given by

$$R_{i, k_i^*} = \log_2(1 + \text{SINR}_{k_i^*}^{\text{BS}_i}). \quad (5)$$

2) *Decoding the CoMP user's signal:* Provided that  $\text{SINR}_{k_i^*}^{\text{BS}_i} \geq \epsilon_i$ , where  $\epsilon_i = 2^{\tilde{R}_{i, k_i^*}} - 1$  and  $\tilde{R}_{i, k_i^*}$  is the data rate of  $\text{U}_{i, k_i^*}$ ,  $\text{BS}_i$  can decode the message sent by  $\text{U}_{i, k_i^*}$  and hence remove this message from its observation successfully. Note that not all base stations can decode the messages from their corresponding NOMA users, which further thins the original HPPP,  $\Phi_c$ . Denote by  $\bar{\Phi}_c$  the new point process including these qualified base stations. Moreover, inviting all the base stations in the plane to participate in CoMP could result in prohibitive system complexity due to the coordination among the qualified base stations. Because of the aforementioned two reasons, it is assumed that only those base stations which can remove their corresponding NOMA users' information and are within disk  $\mathcal{D}$  (which is centered at the origin and with radius  $\mathcal{R}_{\mathcal{D}}$ ), are allowed to participate in CoMP. The modified observation expression after removing the NOMA user's message at  $\text{BS}_i$  can be expressed as follows:

$$\bar{y}_{\text{BS}_i} = \frac{\sqrt{\eta P_0} h_{\text{BS}_i, \text{U}_0}}{\sqrt{L(\|x_i\|)}} s_0 + \sum_{x_j \in \Phi_c \setminus x_i} \frac{\sqrt{\eta P} h_{\text{BS}_i, \text{U}_{j, k_j^*}}}{\sqrt{L(\|y_{j, k_j^*} + x_j - x_i\|)}} s_{j, k_j^*} + n_i. \quad (6)$$

After each base station subtracts its NOMA user's signal from its observation, it forwards its modified observation as well as its NOMA user's message to the network controller.

At the network controller, each forwarded  $\bar{y}_{\text{BS}_i}$  can be further processed by removing the interference term  $s_{j, k_j^*}$ , if  $\text{BS}_j \in \bar{\Phi}_c \cap \mathcal{D}$ , since the network controller has collected those NOMA users' messages. Then  $\bar{y}_{\text{BS}_i}$  can be further rewritten as follows:

$$\tilde{y}_{\text{BS}_i} = \frac{\sqrt{\eta P_0} h_{\text{BS}_i, \text{U}_0}}{\sqrt{L(\|x_i\|)}} s_0 + \sum_{x_j \in \Phi_c \setminus (\bar{\Phi}_c \cap \mathcal{D})} \frac{\sqrt{\eta P} h_{\text{BS}_i, \text{U}_{j, k_j^*}}}{\sqrt{L(\|y_{j, k_j^*} + x_j - x_i\|)}} s_{j, k_j^*} + n_i. \quad (7)$$

For each  $\tilde{y}_{\text{BS}_i}$ , the SINR to decode the CoMP user's message is given by

$$\text{SINR}_0^{\text{BS}_i} = \frac{I_{\text{CoMP}}^U}{\tilde{I}_{\text{inter}}^U + \frac{1}{\rho}}, \quad (8)$$



where

$$\tilde{I}_{\text{inter}}^U = \sum_{x_j \in \Phi_c \setminus (\Phi_c \cap \mathcal{D})} \frac{|h_{\text{BS}_i, \text{U}_{j, k_j^*}}|^2}{L \left( \|y_{j, k_j^*} + x_j - x_i\| \right)}. \quad (9)$$

Finally, the network controller selects the base station which has the largest  $\text{SINR}_0^{\text{BS}_i}$  to decode the CoMP user's message and the corresponding achievable data rate of the CoMP user at the network controller is given by

$$R_0 = \max_{\substack{\text{BS}_i \\ x_i \in \Phi_c \setminus (\Phi_c \cap \mathcal{D})}} \log_2(1 + \text{SINR}_0^{\text{BS}_i}). \quad (10)$$

### III. PERFORMANCE ANALYSIS FOR UPLINK N-NOMA

This section studies the outage probability and the ergodic rate (or average data rate) achieved by the NOMA and CoMP users. The outage probability is the probability of the event that the data rate supported by the instantaneous channel realizations is less than the targeted data rate. Accordingly, the outage probability is an important performance evaluation metric of the quality of service (QoS) in delay-sensitive communication scenarios, where the information sent by the transmitter is at a fixed rate. The average data rate can be used for the case when the transmitted data rates are determined adaptively, according to the users' channel conditions. This case corresponds to delay-tolerant communications. To achieve Shannon's capacity, it is assumed in this paper that the messages sent by users are independently coded with Gaussian codebooks.

#### A. NOMA user

Consider a typical base station in disk  $\mathcal{D}$ , say  $\text{BS}_i$ , we will first study the outage probability for  $\text{BS}_i$  to decode its NOMA user's information which is denoted by  $P_{\text{NOMA}}$ . This probability can be expressed as follows:

$$P_{\text{NOMA}} = \text{P} \left( \text{SINR}_{k_i^*}^{\text{BS}_i} < \epsilon_i \right). \quad (11)$$

Note that  $\text{BS}_i$  is a point in disk  $\mathcal{D}$ , belonging to the HPPP  $\Phi_c$ ; thus it is not hard to conclude that  $\text{BS}_i$  is uniformly distributed in  $\mathcal{D}$  [33].

To calculate the probability  $\text{P} \left( \text{SINR}_{k_i^*}^{\text{BS}_i} < \epsilon_i \right)$ , the first step is to determine the distribution of the composite channel gain,  $\frac{|h_{\text{BS}_i, \text{U}_{i, k}}|^2}{L(\|y_{i, k}\|)}$ . For simplicity of notation, we define  $z_{k, i} \triangleq \frac{|h_{\text{BS}_i, \text{U}_{i, k}}|^2}{L(\|y_{i, k}\|)}$ ,

which means  $z_{k_i^*,i} = \max\{z_{1,i}, \dots, z_{K,i}\}$ . For an unordered channel gain, i.e.,  $z_{k,i}$ , we can apply the Gaussian-Chebyshev approximation as in [7] to obtain the following lemma:

**Lemma 1.** *The cumulative distribution function (CDF) for an unordered composite channel gain, i.e.,  $z_{k,i}$  is given by:*

$$F_{z_{k,i}}(z) \approx \sum_{n=1}^N w_n (1 - e^{-c_n z}), \quad (12)$$

and the corresponding pdf is given by:

$$f_{z_{k,i}}(z) \approx \sum_{n=1}^N w_n c_n e^{-c_n z}, \quad (13)$$

where  $w_n = \frac{\pi}{2N} \sqrt{1 - \theta_n^2} (\theta_n + 1)$ ,  $N$  is the Gaussian-Chebyshev parameter,  $c_n = \left(\frac{R_c}{2}\theta_n + \frac{R_c}{2}\right)^\alpha$ , and  $\theta_n = \cos\left(\frac{2n-1}{2N}\pi\right)$ .

As can be seen in (12), the CDF is expressed as the sum of a finite number of exponentials. It is worth pointing out that this representation not only is accurate with a small  $N$ , but also can significantly facilitate the derivation, as can be seen later in Appendix B.

Another step used to calculate  $P\left(\text{SINR}_{k_i^*}^{\text{BS}_i} < \epsilon_i\right)$  is to determine the Laplace transform for the two interference terms  $I_{\text{CoMP}}^U$  and  $I_{\text{Inter}}^U$ , and the following lemma follows.

**Lemma 2.** *Given the coordinate of  $\text{BS}_i$  at  $x_i$ , the Laplace transform for the interference from the CoMP user is given by:*

$$\begin{aligned} \mathcal{L}_{I_{\text{CoMP}}^U}(s|x_i) &= \mathcal{E}_{I_{\text{CoMP}}^U} \left\{ e^{-sI_{\text{CoMP}}^U} \right\} \\ &= \frac{1}{1 + s\phi L(\|x_i\|)^{-1}}, \end{aligned} \quad (14)$$

and the Laplace transform for the inter-cluster interference is given by:

$$\begin{aligned} \mathcal{L}_{I_{\text{inter}}^U}(s|x_i) &= \mathcal{E}_{I_{\text{inter}}^U} \left\{ e^{-sI_{\text{inter}}^U} \right\} \\ &= \exp\left(-2\pi\lambda_c \frac{s^{\frac{2}{\alpha}}}{\alpha} \mathcal{B}\left(\frac{2}{\alpha}, \frac{\alpha-2}{\alpha}\right)\right), \end{aligned} \quad (15)$$

where  $B(\cdot)$  is the beta function.

*Proof:* Please refer to Appendix A. ■

Note that in Lemma 2, the Laplace transform for  $I_{\text{CoMP}}^U$  is a function of  $\|x_i\|$ . This is due to the fact that the base station which is closer to the CoMP user will be more likely to suffer

strong interference from the CoMP user. But the Laplace transform for  $I_{\text{Inter}}^U$  is not related with  $x_i$ , this is due to the stationary property of the considered Poisson process.

By applying Lemma 1, Lemma 2 and the property of the order statistics [35], the following theorem characterizing the outage probability achieved by  $\text{BS}_i$  to decode  $U_{i,k_i^*}$ 's message is obtained.

**Theorem 1.** *The outage probability achieved by  $\text{BS}_i$  to decode  $U_{i,k_i^*}$ 's message can be approximated as follows:*

$$\begin{aligned} P_{\text{NOMA}} \approx & 1 + \sum_{\substack{k_0+\dots+k_N=K \\ k_0 \neq K}} \binom{K}{k_0, \dots, k_N} \left( \prod_{n=0}^N \tilde{w}_n^{k_n} \right) \times e^{-\mu \epsilon_i \frac{1}{\rho}} \\ & \times \exp \left( -2\pi \lambda_c \frac{(\mu \epsilon_i)^{\frac{2}{\alpha}}}{\alpha} \mathbf{B} \left( \frac{2}{\alpha}, \frac{\alpha-2}{\alpha} \right) \right) \\ & \times \frac{2\mathcal{R}_{\mathcal{D}}^\alpha}{\phi \mu \epsilon_i (2+\alpha)} {}_2F_1 \left( 1, 1 + \frac{2}{\alpha}; 2 + \frac{2}{\alpha}; -\frac{R_{\mathcal{D}}^\alpha}{\phi \mu \epsilon_i} \right), \end{aligned} \quad (16)$$

where  $\tilde{w}_n = -w_n$  for  $1 \leq n \leq N$  and  $\tilde{w}_0 = 1$ , and  $\tilde{c}_n = c_n$  for  $1 \leq n \leq N$  and  $\tilde{c}_0 = 0$ , and  $k_n \geq 0$  for  $0 \leq n \leq N$ , and  $\mu = \sum_{n=0, k_n \neq 0}^N k_n \tilde{c}_n$ , and  $\binom{K}{k_0, \dots, k_N} = \frac{K!}{k_0! \dots k_N!}$ , and  ${}_2F_1(\cdot)$  is the hypergeometric function.

*Proof:* Please refer to Appendix B. ■

The ergodic rate achieved by  $U_{i,k_i^*}$  is given by

$$R_{\text{NOMA}}^{\text{ave}} = \mathcal{E} \left\{ \log_2(1 + \text{SINR}_{k_i^*}^{\text{BS}_i}) \right\}. \quad (17)$$

By applying Theorem 1, we can obtain the following corollary to characterize  $R_{\text{NOMA}}^{\text{ave}}$ .

**Corollary 1.** *The ergodic rate achieved by  $U_{i,k_i^*}$  can be approximated as:*

$$\begin{aligned} R_{\text{NOMA}}^{\text{ave}} \approx & - \sum_{\substack{k_0+\dots+k_N=K \\ k_0 \neq K}} \binom{K}{k_0, \dots, k_N} \frac{2\mathcal{R}_{\mathcal{D}}^\alpha \prod_{n=0}^N \tilde{w}_n^{k_n}}{\ln 2 \phi \mu (2+\alpha)} \int_0^\infty \\ & \frac{e^{-\frac{\mu}{\rho}x}}{x(1+x)} \times \exp \left( -2\pi \lambda_c \frac{(\mu x)^{\frac{2}{\alpha}}}{\alpha} \mathbf{B} \left( \frac{2}{\alpha}, \frac{\alpha-2}{\alpha} \right) \right) \\ & \times {}_2F_1 \left( 1, 1 + \frac{2}{\alpha}; 2 + \frac{2}{\alpha}; -\frac{R_{\mathcal{D}}^\alpha}{\phi \mu x} \right) dx. \end{aligned} \quad (18)$$

*Proof:* Please refer to Appendix C. ■

The use of N-NOMA brings the opportunity for the base stations to serve the corresponding NOMA users, and hence, improves the system throughput. Thus, it is necessary to quantify the ergodic sum rates of the NOMA users. The ergodic sum rate obtained by serving the NOMA users is defined as

$$R_{\text{NOMA}}^{\text{sum}} = \mathcal{E} \left\{ \sum_{x_i \in \Phi_c \cap \mathcal{D}} R_{i,k_i^*} \right\}. \quad (19)$$

Note that here only the NOMA users whose associated base stations are located in disk  $\mathcal{D}$ , are taken into account. A closed-form expression for  $R_{\text{NOMA}}^{\text{sum}}$  is provided as follows.

**Corollary 2.** *The ergodic sum rate for the NOMA users whose associated base stations are located in disk  $\mathcal{D}$  can be calculated as*

$$R_{\text{NOMA}}^{\text{sum}} = \pi \lambda_c \mathcal{R}_{\mathcal{D}}^2 R_{\text{NOMA}}^{\text{ave}}. \quad (20)$$

*Proof:* By using the definition of  $R_{\text{sum}}^{\text{NOMA}}$ , this can be evaluated as:

$$\begin{aligned} R_{\text{sum}}^{\text{NOMA}} &= \mathcal{E} \left\{ \sum_{x_i \in \Phi_c \cap \mathcal{D}} R_{i,k_i^*} \right\} \\ &= \mathcal{E} \{M\} \cdot \mathcal{E} \{R_{i,k_i^*}\} \\ &= \mathcal{E} \{M\} \cdot R_{\text{NOMA}}^{\text{ave}}, \end{aligned} \quad (21)$$

where  $M$  is the number of points in  $\Phi_c \cap \mathcal{D}$ . Note that  $\Phi_c$  is a HPPP, and thus,  $\mathcal{E} \{M\}$  can be expressed as:

$$\mathcal{E} \{M\} = \pi \lambda_c \mathcal{R}_{\mathcal{D}}^2. \quad (22)$$

Therefore, the proof is complete. ■

### B. CoMP user

1) *For the case with adaptive  $\tilde{R}_{i,k_i^*}$ :* In some scenarios, ensuring the QoS of the CoMP user is of the most importance. In this case, in the considered N-NOMA system, the CoMP user can be treated as a primary user and the NOMA user can be treated as a secondary user, as in conventional cognitive networks. Note that, in the conventional OMA based uplink CoMP systems, as in [36], [37], all the base stations in disk  $\mathcal{D}$  are employed to serve the CoMP user and are not allowed to serve any NOMA user. In the considered N-NOMA, if the NOMA users' transmission data rates are adaptively adjusted according to their instantaneous channel

conditions, satisfying  $\tilde{R}_{i,k_i^*} \leq R_{i,k_i^*}$  can ensure that each base station in disk  $\mathcal{D}$  can successfully decode its NOMA user's message. As such, according to the description in Section II, it is easy to conclude that the CoMP user can achieve the same performance in the proposed N-NOMA as in the OMA based system.

2) *For the case with fixed  $\tilde{R}_{i,k_i^*}$ :* It is also interesting to study the case where the NOMA users have fixed data rate requirements. Note that the outage probability achieved by the CoMP user can be expressed as follows:

$$P_{\text{CoMP}} = P \left( \max_{\substack{\text{BS}_i \\ x_i \in \Phi_c \setminus (\bar{\Phi}_c \cap \mathcal{D})}} \text{SINR}_0^{\text{BS}_i} < \epsilon_0 \right) \quad (23)$$

where  $\epsilon_0 = 2^{\tilde{R}_0} - 1$ ,  $\tilde{R}_0$  is the data rates of the CoMP user. In this case, only the base stations which can successfully remove their NOMA users' messages are allowed to participate in CoMP, and the new point process  $\bar{\Phi}_c$  including those qualified base stations can be treated as a thinning process of the original point process  $\Phi_c$ . The outage probability  $P_{\text{NOMA}}$  in Theorem 1 can be treated as a thinning probability of a typical base station. However, this thinning probability is only an average thinning probability of the base stations in disk  $\mathcal{D}$ , over many realizations of the process. As can be expected, the thinning probability of a node will be different in different realizations of the point process. Furthermore, in each realization, the thinning probabilities of different nodes are correlated, since they interfere with each other. The above observations indicate that the analysis for this case will be very challenging. Thus, we will rely on simulations for the performance evaluation for this case, as shown in Section IV. Furthermore, to get insight into this case, we consider a simplified N-NOMA scheme, referred to as the nearest N-NOMA scheme, as shown in the following subsection.

### C. Nearest N-NOMA scheme

In the nearest N-NOMA scheme, only one base station, which is nearest to the CoMP user, is invited to apply NOMA to serve the CoMP user and its NOMA user simultaneously. Similar to the aforementioned general N-NOMA scheme, in the nearest N-NOMA scheme, the nearest base station first tries to decode its NOMA user's message. If successfully, the nearest base station will then subtract the NOMA users signal from its observation, and deliver the remaining signal to the network controller.

Besides the aforementioned motivation in Section III-B, it is worth pointing out that there is another motivation to study the nearest N-NOMA scheme. The nearest N-NOMA scheme

needs only one base station to serve the CoMP user, and hence, the system overhead is reduced. Accordingly the nearest N-NOMA scheme is applicable to scenarios where the system overhead is the bottleneck of the system performance.

In the following, the outage performance of the nearest N-NOMA scheme is analyzed. For notation convenience, in this subsection, the base stations are ordered according to their distances to the CoMP user as follows:

$$L(|x_i|) \leq L(|x_j|) \quad (24)$$

for  $i < j$ . Thus, the nearest base station is  $BS_1$ .

1) *NOMA user*: Note that according to [33],  $BS_1$  is not a typical point since it is closest to the CoMP user. Thus, the NOMA user's outage probability for the nearest N-NOMA scheme will be different from the outage probability obtained in Theorem 1, as highlighted in the following proposition.

**Proposition 1.** *When  $\alpha = 4$ , the NOMA user's outage probability for the nearest N-NOMA scheme can be approximated as follows:*

$$\begin{aligned} P_1^{nearest} \approx & 1 + \sum_{\substack{k_0 + \dots + k_N = K \\ k_0 \neq K}} \binom{K}{k_0, \dots, k_N} \prod_{n=0, k_n \neq 0}^N \tilde{w}_n^{k_n} e^{-k_n \tilde{c}_n \epsilon_1 \frac{1}{\rho}} \\ & \times \exp\left(-2\pi\lambda_c \frac{(\epsilon_1 \mu)^{\frac{2}{\alpha}}}{\alpha} B\left(\frac{2}{\alpha}, \frac{\alpha-2}{\alpha}\right)\right) \times \\ & \int_0^\infty \exp\left(\frac{1}{2}\pi\lambda_c \sqrt{\epsilon_1 \mu} \arctan\left(\sqrt{-\frac{1}{2} + \frac{1}{2}\sqrt{1 + \frac{16d^4}{\epsilon_1 \mu}}}\right)\right) \\ & \times \frac{1}{1 + \phi \epsilon_1 \mu d^{-4}} \times 2\lambda_c \pi d e^{-\lambda_c \pi d^2} dd. \end{aligned} \quad (25)$$

*Proof:* Please refer to Appendix D. ■

2) *CoMP user*: When the NOMA user's rate is fixed, the outage probability achieved by the CoMP user is characterized as shown in the following proposition.

**Proposition 2.** *When  $\alpha = 4$ , the CoMP user's outage probability for the nearest N-NOMA*

scheme can be approximated as follows:

$$\begin{aligned}
P_0^{nearest} \approx & 1 + \sum_{\substack{k_0 + \dots + k_N = K \\ k_0 \neq K}} \binom{K}{k_0, \dots, k_N} \prod_{n=0, k_n \neq 0}^N \tilde{w}_n^{k_n} e^{-k_n \tilde{c}_n \epsilon_1 \frac{1}{\rho}} \\
& \times \int_0^\infty \exp \left( -2\pi \lambda_c \frac{\xi(d)^{\frac{2}{\alpha}}}{\alpha} \mathbf{B} \left( \frac{2}{\alpha}, \frac{\alpha - 2}{\alpha} \right) \right. \\
& \quad \left. + \frac{1}{2} \pi \lambda_c \sqrt{\xi(d)} \arctan \left( \sqrt{-\frac{1}{2} + \frac{1}{2} \sqrt{1 + \frac{16d^4}{\xi(d)}}} \right) \right) \\
& \times \frac{2\pi \lambda_c d^5}{\phi \epsilon_1 \mu + d^4} \exp \left( -\frac{\epsilon_0 (\phi \epsilon_1 \mu + d^4)}{\phi \rho} - \lambda_c \pi d^2 \right) dd,
\end{aligned} \tag{26}$$

where  $\xi(d) = \epsilon_1 \mu + \epsilon_0 (\phi \epsilon_1 \mu + d^4) / \phi$ .

*Proof:* Please refer to Appendix D. ■

**Remark 1.** We choose  $\alpha = 4$  without loss of generality, as the procedure of the analysis is the same. In addition, the geometry property that the distance between the BSs is much larger than that between a NOMA user to its associated BS is used to facilitate analysis, as shown in Appendix E.

#### IV. NUMERICAL RESULTS

In this section, computer simulations are performed to demonstrate the performance of the proposed N-NOMA system and also verify the accuracy of the analytical results. The thermal noise power is set to  $-170$  dBm/Hz, the carrier frequency is  $f_c = 2 \times 10^9$  Hz, the transmission bandwidth is  $B = 10$  MHz, and the transmitter and receiver antenna gains are set to 1. The path loss exponent is set as  $\alpha = 4$ . The path loss parameter is set as  $\eta = \frac{c^2}{16\pi^2 f_c^2}$ , where  $c$  is the light speed.

In Fig. 2 and Fig. 3, the outage probability of a typical NOMA user is studied. Fig. 2 shows the outage probability as a function of the user target rate, while Fig. 3 shows it as a function of the NOMA user transmission power. It should be mentioned that the average outage probabilities of the NOMA users, whose associated base stations are located in disk  $\mathcal{D}$ , are considered in both figures. The radius of  $\mathcal{D}$  is set as  $\mathcal{R}_{\mathcal{D}} = 500$  m. As shown in Figs. 2 and 3, computer simulations perfectly match the theoretical results, which demonstrates the accuracy of the developed analysis. From Fig. 2, it is can be seen that as the number of users in a cluster increases, the outage

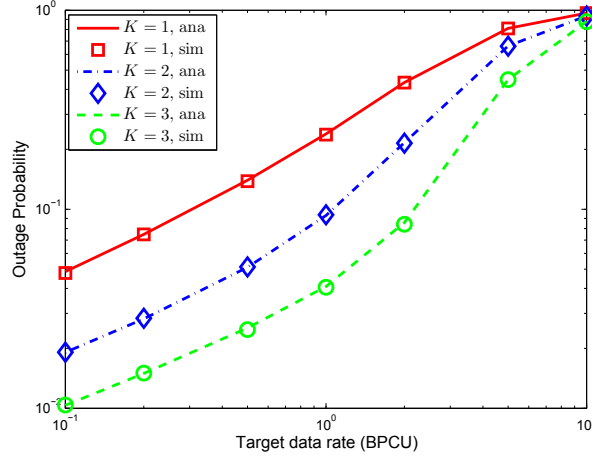


Fig. 2: NOMA user outage probability versus target data rate.  $\mathcal{R}_c = 50$  m,  $\lambda_c = 2 \times 10^{-5}/m^2$ ,  $P = 0.1$  W,  $\phi = 10$ , and the Gaussian-Chebyshev parameter  $N = 20$ . Notations, sim: simulation results; ana: analytical results.

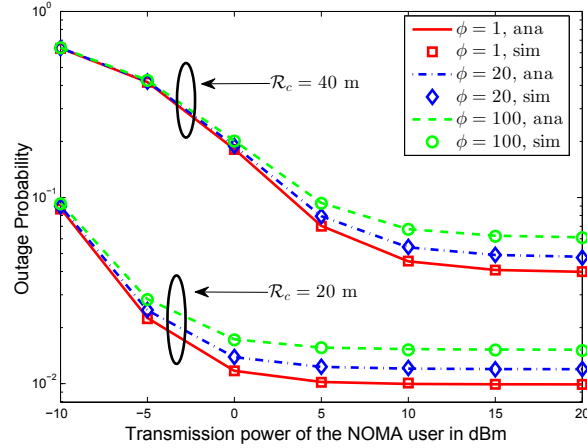


Fig. 3: NOMA user outage probability versus transmission power.  $K = 2$ ,  $\tilde{R}_{i,k_i^*} = 1$  bit per channel use (BPCU),  $\lambda_c = 2 \times 10^{-5}/m^2$ , and the Gaussian-Chebyshev parameter  $N = 20$ .

probability of the NOMA user decreases. This is because the NOMA user is chosen from the  $K$  users in the cluster according to the channel conditions. From Fig. 3, it is shown that as the transmission power of the CoMP user increases, the outage probability of a NOMA user also increases. The reason is that when decoding the NOMA user's message, the CoMP user's message is treated as noise. From Fig. 3 it is also seen that the outage probability of a NOMA user increases with the radius of a cluster.

Fig. 4(a) shows the ergodic rate of a typical NOMA user whose associated base station is



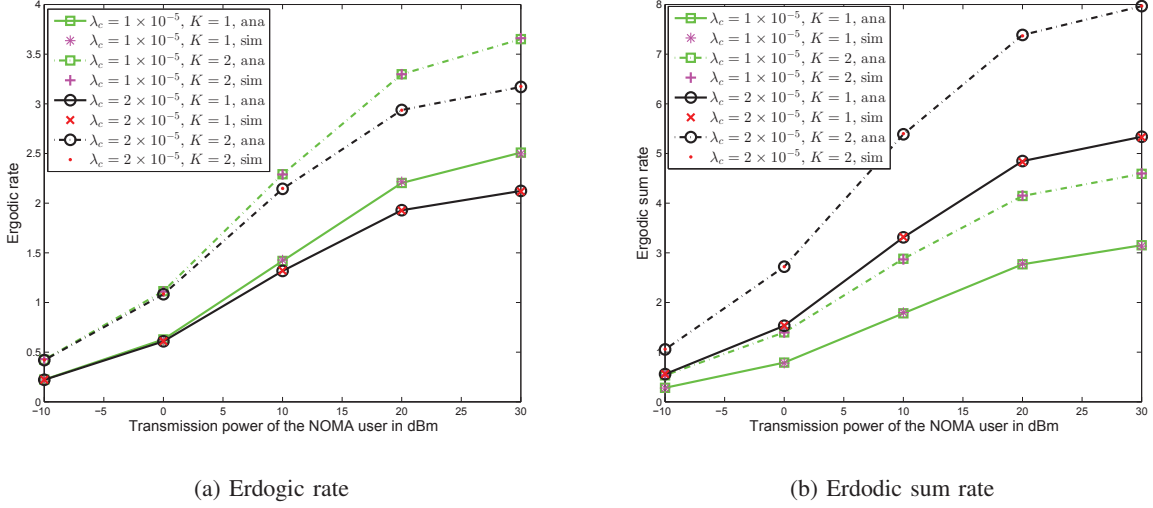


Fig. 4: The ergodic rate and ergodic sum rate of the NOMA users.  $\mathcal{R}_c = 80$  m,  $\phi = 10$ , and the Gaussian-Chebyshev parameter  $N = 20$ .

located in disk  $\mathcal{D}$  and Fig. 4(b) shows the ergodic sum rate of the NOMA users whose associated base stations are located in disk  $\mathcal{D}$ . The radius of  $\mathcal{D}$  is set as  $\mathcal{R}_D = 200$  m in Figs. 4(a) and 4(b). Both the rate of a typical NOMA user and the sum rate of the NOMA users increase with  $K$ , as shown in the figures. This observation is consistent with the results shown in Fig. 2. It is obvious that as the density of cells increases, the performance of a NOMA user decreases, due to the enhanced inter-cell interferences. This statement is validated in Fig. 4(a). Interestingly, on the other hand, as the density of cells increases, there will be more NOMA users which can be served with their associated base stations located in disk  $\mathcal{D}$ , which offer opportunity to improve the sum rate, as shown in Fig. 4(b). Thus, there is a tradeoff between the single user's QoS and system throughput.

Fig. 5 shows the CoMP user's outage performance, where the NOMA users' data rates are fixed. The CoMP user's data rate is set as  $\tilde{R}_0 = 1$  BPCU. Note that the outage probability achieved by the CoMP user is dependent on the NOMA users' data rates, because prior to decoding the CoMP user's message, the base stations need to decode their NOMA users' messages. This is consistent with the observation from Fig. 5, where as the rates of NOMA users increase, the outage performance achieved by the CoMP user degrades. Another interesting observation is that when  $\lambda = 1 \times 10^{-5}$ , the gap between the two cases with different NOMA users' data rates is fairly small. This can be easily explained, as when  $\lambda$  is small, the main

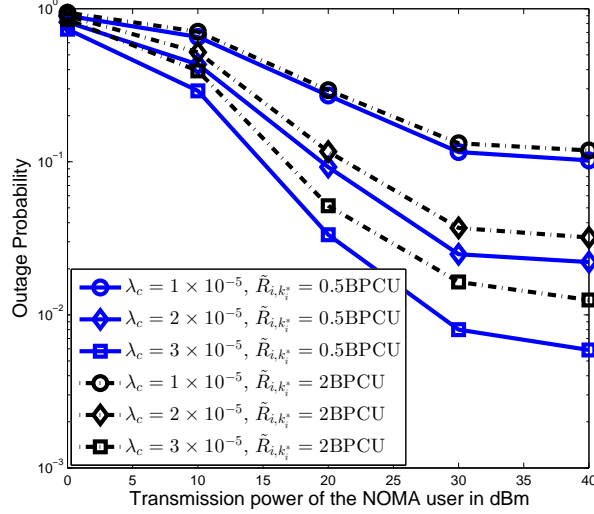


Fig. 5: CoMP user's outage performance.  $\mathcal{R}_D = 300$  m,  $\mathcal{R}_c = 40$  m,  $\phi = 20$ ,  $K = 3$ .

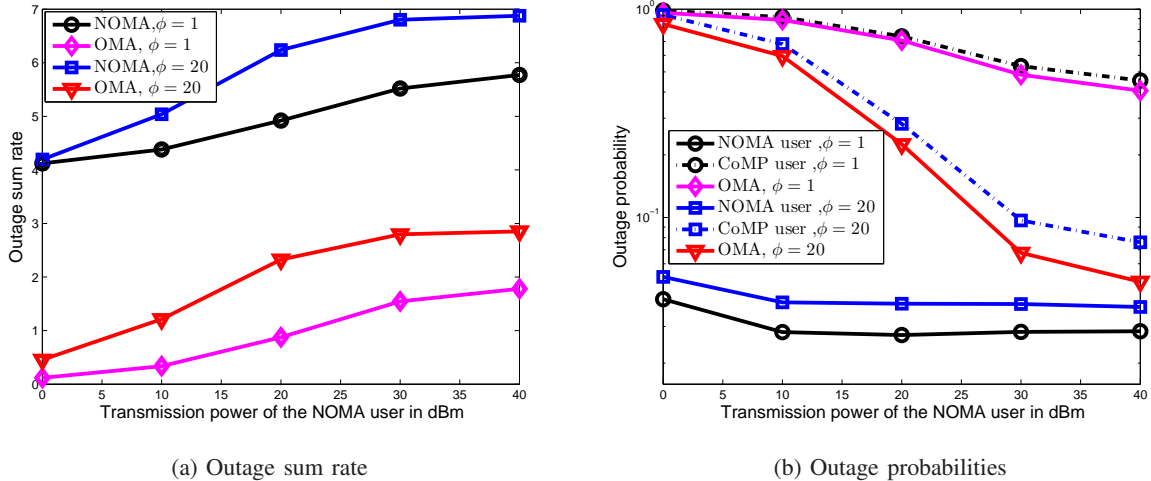


Fig. 6: Performance comparison between N-NOMA and OMA in terms of the outage sum rate.  $K = 3$ ,  $\tilde{R}_{i,k_i^*} = 0.5$  BPCU,  $\tilde{R}_0 = 3$  BPCU,  $\lambda_c = 3 \times 10^{-5}/m^2$ ,  $\mathcal{R}_c = 40$  m,  $\mathcal{R}_D = 300$  m.

limitation of the CoMP user's performance is the number of serving base stations.

Figs. 6 and 7 show the performance comparison between the proposed N-NOMA scheme and the OMA scheme. Note that in the benchmark OMA scheme, only the CoMP user is served by the base stations in disk  $\mathcal{D}$ . More specifically, in the benchmark OMA scheme, if one of the base stations in disk  $\mathcal{D}$  can successfully decode the CoMP user's message through its observation, then the CoMP user is not in outage. Fig. 6(a) shows the performance comparison in terms of the outage sum rate, where the transmission data rates of the users are fixed, while the

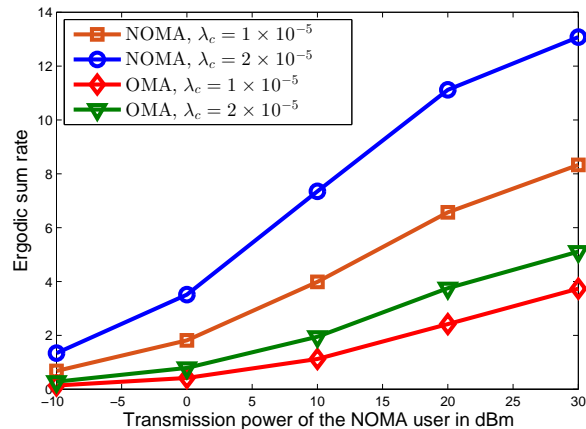


Fig. 7: Performance comparison between N-NOMA and OMA in terms of the ergodic sum rate.  $K = 2$ ,  $\phi = 10$ ,  $\mathcal{R}_c = 80$  m,  $\mathcal{R}_D = 200$  m.

corresponding outage probabilities are shown in Fig. 6(b). As shown in Fig. 6(a), the proposed N-NOMA scheme outperforms OMA. For example, when the transmission power of the NOMA user and the CoMP user is 30 dBm, the outage sum rate achieved by the OMA scheme is about 1.8 BPCU, while the proposed N-NOMA supports about 5.7 BPCU. Hence, the N-NOMA scheme has an extra gain of 3.9 BPCU compared to OMA. In addition, the proposed N-NOMA scheme also outperforms OMA in terms of the ergodic sum rate, as shown in Fig. 7. Note that, in Fig. 7, the rates of the NOMA users are adaptively adjusted according to the instantaneous channel conditions as described in Section III. B; thus the CoMP user in the proposed N-NOMA scheme can achieve the same data rates as in the benchmark OMA scheme. Hence, as shown in Fig. 7, we conclude that the proposed N-NOMA scheme can achieve higher data rates than the benchmark OMA scheme by serving those extra NOMA users, while not degrading the CoMP user's performance.

Figs. 8 and 9 demonstrate the performance of the nearest N-NOMA scheme. Fig. 8 shows the outage performance achieved by the NOMA and the CoMP users, and simulations validate the accuracy of the analysis presented in Proposition 1 and Proposition 2. It is shown in Fig. 8 that in the proposed nearest N-NOMA scheme, the outage probability achieved by the CoMP user is always larger than that of the NOMA user. This is because only after the NOMA user's message is decoded, the CoMP user's message can be decoded. It is also observed in Figs. 8(a) and 8(b) that increasing the transmission power of the CoMP user and reducing the data rate of the NOMA user can improve the CoMP user's performance. However, this is at the expense of

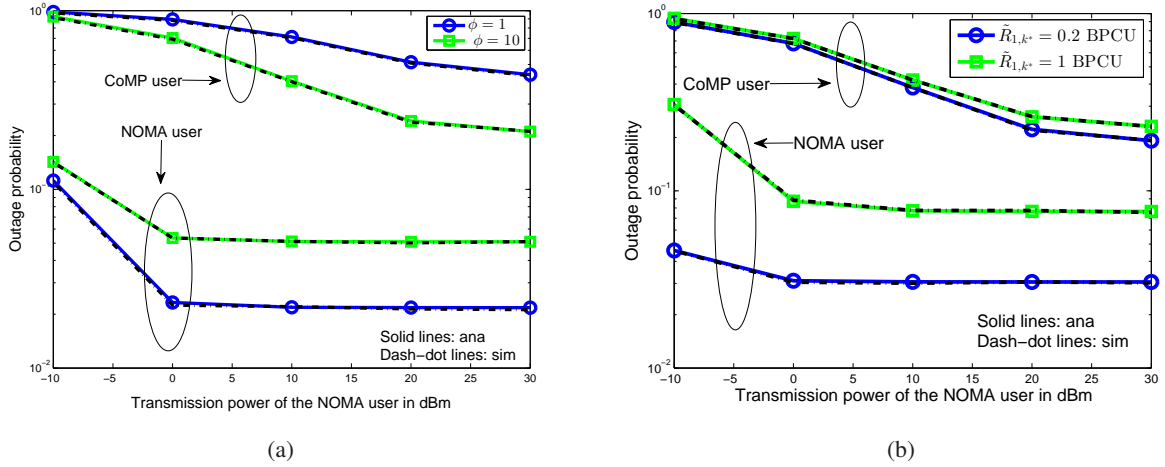


Fig. 8: Outage probabilities achieved by the nearest N-NOMA scheme.  $K = 3$ ,  $\mathcal{R}_c = 30$  m,  $\lambda_c = 3 \times 10^{-5}/m^2$ ,  $\tilde{R}_0 = 0.5$  BPCU (a)  $\tilde{R}_{1,k_1^*} = 0.5$  BPCU (b)  $\phi = 10$ .

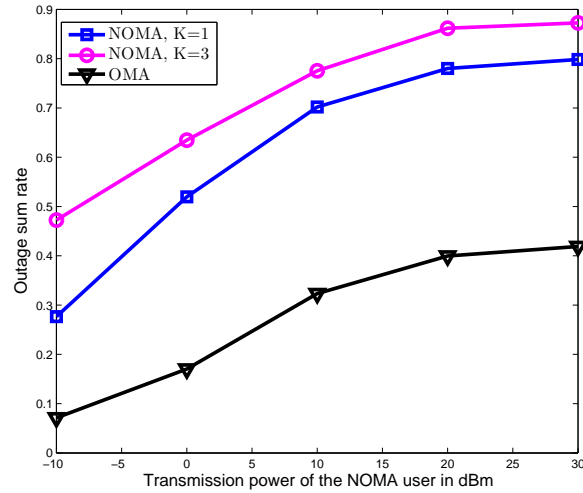


Fig. 9: Comparison between the nearest N-NOMA scheme and OMA.  $\mathcal{R}_c = 30$  m,  $\lambda_c = 3 \times 10^{-5}/m^2$ ,  $\tilde{R}_0 = 0.5$  BPCU,  $\tilde{R}_{1,k_1^*} = 0.5$  BPCU,  $\phi = 10$ .

degrading the NOMA user's performance. From Fig. 8, it can be observed that the performance of the CoMP user is very poor in the nearest N-NOMA scheme. This is because only one base station is employed to serve the CoMP user. This observation reveals the importance of inviting multiple base stations to participate in CoMP. In Fig. 9, the nearest N-NOMA scheme is compared with the OMA scheme, where the nearest base station is chosen to serve the CoMP user, and only this user is served. As shown in the figure, NOMA outperforms OMA in terms

of the outage sum rate and the gap between NOMA and OMA increases with  $K$ .

## V. CONCLUSIONS

In this paper, in order to improve the system throughput and spectral efficiency, we have proposed an uplink N-NOMA scheme for the CoMP transmission. In the proposed scheme, a CoMP user and multiple NOMA users are served simultaneously. To get insight into the problem, a PCP model has been introduced to characterize the locations of the nodes. The outage probabilities and ergodic rates of the users have been analyzed to evaluate the performance of the proposed N-NOMA scheme. Closed-form expressions for the outage probabilities and the sum rates have been developed, and also validated by computer simulations. Extensive numerical results have been presented to demonstrate the performance of the proposed N-NOMA scheme. Comparisons with the OMA scheme have been presented, which demonstrate that N-NOMA can significantly improve the system throughput and spectral efficiency.

### APPENDIX A

#### PROOF FOR LEMMA 2

Recall that  $I_{\text{CoMP}}^U = \frac{\phi |h_{\text{BS}_i, \text{U}_0}|^2}{L(\|x_i\|)}$ . Therefore, the expectation for the CoMP interference can be simply calculated as follows:

$$\begin{aligned} \mathcal{L}_{I_{\text{CoMP}}^U}(s|x_i) &= \mathcal{E}_{I_{\text{CoMP}}^U} \left\{ e^{-s I_{\text{CoMP}}^U} \right\} \\ &= \int_0^\infty e^{-s \frac{\phi x}{L(\|x_i\|)}} e^{-x} dx \\ &= \frac{1}{1 + s\phi L(\|x_i\|)^{-1}}, \end{aligned} \quad (27)$$

which follows from the fact that  $h_{\text{BS}_i, \text{U}_0}$  is Rayleigh distributed.

We can evaluate  $\mathcal{L}_{I_{\text{inter}}^U}(s|x_i)$  as

$$\mathcal{L}_{I_{\text{inter}}^U}(s|x_i) = \mathcal{E} \left\{ \prod_{x_j \in \Phi_c \setminus x_i} \exp \left( -s \frac{|h_{\text{BS}_i, \text{U}_{j, k_j^*}}|^2}{L(\|y_{j, k_j^*} + x_j - x_i\|)} \right) \right\},$$

where the arguments for the expectation include  $h_{\text{BS}_i, \text{U}_{j, k_j^*}}$  and the locations of  $\text{BS}_i$ ,  $\text{BS}_j$  and  $\text{U}_{j, k_j^*}$ . Note that  $h_{\text{BS}_i, \text{U}_{j, k_j^*}}$  is independent from  $\|y_{j, k_j^*} + x_j - x_i\|$ . Therefore, by using the assumption that  $h_{\text{BS}_i, \text{U}_{j, k_j^*}}$  is independently and identically Rayleigh distributed, we have

$$\mathcal{L}_{I_{\text{inter}}^U}(s) = \mathcal{E} \left\{ \prod_{x_j \in \Phi_c \setminus x_i} \frac{1}{\frac{s}{L(\|y_{j, k_j^*} + x_j - x_i\|)} + 1} \right\}. \quad (28)$$

By applying the Campbell's theorem and the probability generating functional (PGFL) [33], we have

$$\mathcal{L}_{I_{\text{inter}}^U}(s) = \exp \left( -\lambda_c \int_{R^2} \left( 1 - \mathcal{E}_{y_j, k_j^*} \left\{ \frac{1}{\frac{s}{L(\|y_j, k_j^* + x - x_i\|)} + 1} \right\} \right) dx \right). \quad (29)$$

Denote the pdf of  $y_j, k_j^*$  by  $f_{y_j, k_j^*}(y)$ , and the Laplace transform is expressed as follows:

$$\mathcal{L}_{I_{\text{inter}}^U}(s) = \exp \left( -\lambda_c \int_{R^2} f_{y_j, k_j^*}(y) \int_{R^2} \left( 1 - \frac{1}{\frac{s}{L(\|y + x - x_i\|)} + 1} \right) dx dy \right). \quad (30)$$

Using the substitution  $y + x - x_i \rightarrow x'$ , we have

$$\begin{aligned} \mathcal{L}_{I_{\text{inter}}^U}(s) &= \exp \left( -\lambda_c \int_{R^2} f_{y_j, k_j^*}(y) \int_{R^2} \left( 1 - \frac{1}{\frac{s}{L(\|x'\|)} + 1} \right) dx' dy \right) \\ &\stackrel{(a)}{=} \exp \left( -\lambda_c \int_{R^2} f_{y_j, k_j^*}(y) 2\pi \int_0^\infty \left( 1 - \frac{1}{\frac{s}{L(r)} + 1} \right) r dr dy \right), \end{aligned} \quad (31)$$

where (a) follows from changing to polar coordinates.

Further, by applying the Beta function, we have

$$\begin{aligned} \mathcal{L}_{I_{\text{inter}}^U}(s) &\stackrel{(a)}{=} \exp \left( -\lambda_c \int_{R^2} f_{y_j, k_j^*}(y) 2\pi \frac{s^{\frac{2}{\alpha}}}{\alpha} \mathbf{B} \left( \frac{2}{\alpha}, \frac{\alpha - 2}{\alpha} \right) dy \right) \\ &\stackrel{(b)}{=} \exp \left( -2\pi \lambda_c \frac{s^{\frac{2}{\alpha}}}{\alpha} \mathbf{B} \left( \frac{2}{\alpha}, \frac{\alpha - 2}{\alpha} \right) \right), \end{aligned} \quad (32)$$

where (a) follows from the fact that the integral with respect to  $r$  is not a function of  $y$ , and (b) follows from the fact that  $\int_{R^2} f_{y_j, k_j^*}(y) dy = 1$ . The use of other user selection strategies does not affect much the results for the Laplace of the interference. Please note that  $\alpha$  cannot be chosen to be 2.

Therefore Lemma 2 is proved.

## APPENDIX B

### PROOF FOR THEOREM 1

The SINR to decode  $U_{i, k_i^*}$ 's message can be expressed as follows:

$$\text{SINR}_{k_i^*}^{\text{BS}_i} = \frac{z_{k_i^*, i}}{I_{\text{CoMP}}^U + I_{\text{inter}}^U + \frac{1}{\rho}}. \quad (33)$$

Since the Laplace transform for  $I_{\text{CoMP}}^U$  is a function of  $\|x_i\|$ , we first fix the location of  $\text{BS}_i$  and calculate the conditioned outage probability:

$$\begin{aligned} P_{\text{NOMA}}(x_i) &= \text{P} \left( \text{SINR}_{k_i^*}^{\text{BS}_i} < \epsilon_i | x_i \right) \\ &= \text{P} \left( z_{k_i^*,i} < \epsilon_i \left( I_{\text{CoMP}}^U + I_{\text{inter}}^U + \frac{1}{\rho} \right) \right) \\ &= \mathcal{E}_{I_{\text{CoMP}}^U, I_{\text{inter}}^U} \left\{ \left( \text{P} \left( z_{k,i} < \epsilon_i \left( I_{\text{CoMP}}^U + I_{\text{inter}}^U + \frac{1}{\rho} \right) \right) \right)^K \right\}, \end{aligned} \quad (34)$$

where the last step follows from the fact that  $z_{k_i^*,i}$  is largest in  $\{z_{1,i}, \dots, z_{K,i}\}$ . By applying the approximated expression for the pdf of  $z_{k,i}$  as shown in Lemma 1, we have

$$\begin{aligned} P_{\text{NOMA}}(x_i) & \\ &\approx \mathcal{E}_{I_{\text{CoMP}}^U, I_{\text{inter}}^U} \left\{ \left( \sum_{n=1}^N w_n \left( 1 - e^{-c_n \epsilon_i (I_{\text{CoMP}}^U + I_{\text{inter}}^U + \frac{1}{\rho})} \right) \right)^K \right\} \\ &= \mathcal{E}_{I_{\text{CoMP}}^U, I_{\text{inter}}^U} \left\{ \left( \sum_{n=1}^N w_n - \sum_{n=1}^N w_n e^{-c_n \epsilon_i (I_{\text{CoMP}}^U + I_{\text{inter}}^U + \frac{1}{\rho})} \right)^K \right\} \\ &\approx \mathcal{E}_{I_{\text{CoMP}}^U, I_{\text{inter}}^U} \left\{ \left( 1 - \sum_{n=1}^N w_n e^{-c_n \epsilon_i (I_{\text{CoMP}}^U + I_{\text{inter}}^U + \frac{1}{\rho})} \right)^K \right\}. \end{aligned} \quad (35)$$

Define  $\tilde{w}_n = -w_n$  for  $1 \leq n \leq N$  and  $\tilde{w}_0 = 1$ . In addition,  $\tilde{c}_n = c_n$  for  $1 \leq n \leq N$  and  $\tilde{c}_0 = 0$ .

Applying the multinomial theorem, we expand the expression as follows:

$$\begin{aligned} P_{\text{NOMA}}(x_i) &\approx 1 + \sum_{\substack{k_0 + \dots + k_N = K \\ k_0 \neq K}} \binom{K}{k_0, \dots, k_N} \prod_{n=0, k_n \neq 0}^N \tilde{w}_n^{k_n} e^{-k_n \tilde{c}_n \epsilon_i \frac{1}{\rho}} \\ &\quad \times \mathcal{E}_{I_{\text{CoMP}}^U} \left\{ e^{-\mu \epsilon_i I_{\text{CoMP}}^U} | x_i \right\} \mathcal{E}_{I_{\text{inter}}^U} \left\{ e^{-\mu \epsilon_i I_{\text{inter}}^U} | x_i \right\}, \end{aligned} \quad (36)$$

where  $\mu = \sum_{n=0, k_n \neq 0}^N k_n \tilde{c}_n$ ,  $\binom{K}{k_0, \dots, k_N} = \frac{K!}{k_0! \dots k_N!}$ .

By applying the Laplace transform for  $I_{\text{CoMP}}^U$  and  $I_{\text{inter}}^U$  obtained in Lemma 2, the conditioned outage probability can be expressed as

$$\begin{aligned} P_{\text{NOMA}}(x_i) &\approx 1 + \sum_{\substack{k_0 + \dots + k_N = K \\ k_0 \neq K}} \binom{K}{k_0, \dots, k_N} \prod_{n=0, k_n \neq 0}^N \tilde{w}_n^{k_n} e^{-k_n \tilde{c}_n \epsilon_i \frac{1}{\rho}} \\ &\quad \times \frac{\exp \left( -2\pi \lambda_c \frac{\mu \frac{2}{\alpha}}{\alpha} \mathbf{B} \left( \frac{2}{\alpha}, \frac{\alpha-2}{\alpha} \right) \right)}{1 + \phi \mu L (\|x_i\|)^{-1}}. \end{aligned} \quad (37)$$

Note that  $x_i$  is uniformly distributed in disk  $\mathcal{D}$ , for the reason that we have conditioned on  $x_i \in \Phi_c \cap \mathcal{D}$ . Thus, the outage probability  $P_{\text{NOMA}}$  can be calculated as follows:

$$\begin{aligned}
P_{\text{NOMA}} &= \frac{1}{\pi \mathcal{R}_{\mathcal{D}}^2} \int_{x_i \in \mathcal{D}} P_{\text{NOMA}}(x_i) dx_i \\
&\stackrel{(a)}{=} 1 + \frac{2}{\mathcal{R}_{\mathcal{D}}^2} \sum_{\substack{k_0 + \dots + k_N = K \\ k_0 \neq K}} \binom{K}{k_0, \dots, k_N} \prod_{n=0, k_n \neq 0}^N \tilde{w}_n^{k_n} \\
&\quad \times e^{-k_n \tilde{c}_n \epsilon_i \frac{1}{\rho}} \exp \left( -2\pi \lambda_c \frac{\mu_c^{\frac{2}{\alpha}}}{\alpha} \mathbf{B} \left( \frac{2}{\alpha}, \frac{\alpha - 2}{\alpha} \right) \right) \\
&\quad \times \int_0^{R_{\mathcal{D}}} \frac{1}{1 + \phi \mu r^{-\alpha}} r dr,
\end{aligned} \tag{38}$$

where (a) follows from changing to polar coordinates. Finally, by applying the hypergeometric function, Theorem 1 is proved.

## APPENDIX C

### PROOF FOR COROLLARY 1

$$\begin{aligned}
R_{\text{NOMA}}^{\text{ave}} &= \mathcal{E} \left\{ \log_2(1 + \text{SINR}_{k_i^*}^{\text{BS}_i}) \right\} \\
&\stackrel{(a)}{=} \int_0^\infty \mathbb{P} \left( \log_2(1 + \text{SINR}_{k_i^*}^{\text{BS}_i}) > t \right) dt \\
&= \int_0^\infty \mathbb{P} \left( \text{SINR}_{k_i^*}^{\text{BS}_i} > 2^t - 1 \right) dt \\
&= \int_0^\infty 1 - \mathbb{P} \left( \text{SINR}_{k_i^*}^{\text{BS}_i} < 2^t - 1 \right) dt \\
&\stackrel{(b)}{=} \frac{1}{\ln 2} \int_0^\infty \frac{1 - \mathbb{P} \left( \text{SINR}_{k_i^*}^{\text{BS}_i} < x \right)}{1 + x} dx,
\end{aligned} \tag{39}$$

where (a) is obtained as  $\mathcal{E}\{x\} = \int_{t>0} \mathbb{P}(X > t) dt$  for a positive random variable  $X$  and it is obvious that  $\log_2(1 + \text{SINR}_{k_i^*}^{\text{BS}_i})$  is a positive random variable, and (b) follows from  $x = 2^t - 1$ .

After some manipulations, Corollary 1 is obtained.

## APPENDIX D

### A. Proof for Proposition 1

Denote the distance between the CoMP user to its nearest BS as  $d$ , i.e.,  $d = L(\|x_1\|)$ . We first consider the case when the value of  $d$  is fixed.



Given a fixed  $d$ , the Laplace transform of interference from the other NOMA users can be expressed as

$$\mathcal{L}_{I_{\text{inter}}^U}(s) = \mathcal{E} \left\{ \prod_{x_j \in \Phi_c \setminus x_1} \frac{1}{\frac{s}{L(\|y_{j,k_j^*} + x_j - x_1\|)} + 1} \right\}. \quad (40)$$

Again, by applying the Campbell's theorem and the PGFL [33], the following expression is obtained

$$\mathcal{L}_{I_{\text{inter}}^U}(s) = \exp \left( -\lambda_c \int_{\|x\| > d^2} \left( 1 - \mathcal{E}_{y_{j,k_j^*}} \left\{ \frac{1}{\frac{s}{L(\|y_{j,k_j^*} + x - x_1\|)} + 1} \right\} \right) dx \right). \quad (41)$$

Note that in (41), the integral region is changed compared to (29), which makes the calculation more challenging, because the effect of  $y_{j,k_j^*}$  cannot be removed from (41) as in (29).

A closed-form expression for  $\mathcal{E}_{y_{j,k_j^*}} \left\{ \frac{1}{\frac{s}{L(\|y_{j,k_j^*} + x - x_1\|)} + 1} \right\}$ , when  $K = 1$ , can be obtained using a geometric probability approach as in [14], [38]. However, for  $K > 1$ , the calculation of  $\mathcal{E}_{y_{j,k_j^*}} \left\{ \frac{1}{\frac{s}{L(\|y_{j,k_j^*} + x - x_1\|)} + 1} \right\}$  is very challenging. Hence, making reasonable approximations to simplify the calculation is necessary. Note that when the distance between the BSs is much larger than that between a NOMA user and its associated BS, the impact of  $y_{j,k_j^*}$  can be omitted. Taking  $\alpha = 4$ ,  $\mathcal{L}_{I_{\text{inter}}^U}(s)$  can be approximated as:

$$\mathcal{L}_{I_{\text{inter}}^U}(s) \approx \exp \left( -2\pi\lambda_c \frac{s^{\frac{2}{\alpha}}}{\alpha} \mathbf{B} \left( \frac{2}{\alpha}, \frac{\alpha - 2}{\alpha} \right) \right. \quad (42)$$

$$\left. + \frac{1}{2}\pi\lambda_c \sqrt{s} \arctan \left( \sqrt{-\frac{1}{2} + \frac{1}{2}\sqrt{1 + \frac{16d^4}{s}}} \right) \right). \quad (43)$$

Then, by using similar steps as in Appendix B, the outage probability of the nearest BS's NOMA

user given a fixed  $d$  and fixed  $|h_{\text{BS}_i, \text{U}_0}|$  can be approximated as follows:

$$\begin{aligned}
& P_1^{\text{nearest}}(d, |h_{\text{BS}_i, \text{U}_0}|) \\
& \approx 1 + \sum_{\substack{k_0 + \dots + k_N = K \\ k_0 \neq K}} \binom{K}{k_0, \dots, k_N} \prod_{n=0, k_n \neq 0}^N \tilde{w}_n^{k_n} e^{-k_n \tilde{c}_n \epsilon_1^{\frac{1}{\rho}}} \\
& \times \exp \left( -2\pi \lambda_c \frac{(\epsilon_1 \mu)^{\frac{2}{\alpha}}}{\alpha} \mathbf{B} \left( \frac{2}{\alpha}, \frac{\alpha - 2}{\alpha} \right) \right. \\
& \quad \left. + \frac{1}{2} \pi \lambda_c \sqrt{\epsilon_1 \mu} \arctan \left( \sqrt{-\frac{1}{2} + \frac{1}{2} \sqrt{1 + \frac{16d^4}{\epsilon_1 \mu}}} \right) \right) \\
& \times \exp \left( -\frac{\phi \epsilon_1 \mu |h_{\text{BS}_i, \text{U}_0}|^2}{d^4} \right).
\end{aligned} \tag{44}$$

After taking the average over  $h_{\text{BS}_i, \text{U}_0}$ , the outage probability of the nearest BS's NOMA user given a fixed  $d$  can be approximated as:

$$\begin{aligned}
& P_1^{\text{nearest}}(d) \approx 1 + \sum_{\substack{k_0 + \dots + k_N = K \\ k_0 \neq K}} \binom{K}{k_0, \dots, k_N} \prod_{n=0, k_n \neq 0}^N \tilde{w}_n^{k_n} e^{-k_n \tilde{c}_n \epsilon_1^{\frac{1}{\rho}}} \\
& \times \exp \left( -2\pi \lambda_c \frac{(\epsilon_1 \mu)^{\frac{2}{\alpha}}}{\alpha} \mathbf{B} \left( \frac{2}{\alpha}, \frac{\alpha - 2}{\alpha} \right) \right. \\
& \quad \left. + \frac{1}{2} \pi \lambda_c \sqrt{\epsilon_1 \mu} \arctan \left( \sqrt{-\frac{1}{2} + \frac{1}{2} \sqrt{1 + \frac{16d^4}{\epsilon_1 \mu}}} \right) \right) \\
& \times \frac{1}{1 + \phi \epsilon_1 \mu d^{-4}}.
\end{aligned} \tag{45}$$

Note that the pdf of  $L(\|x_1\|)$  [33] can be expressed as

$$f_{L(\|x_1\|)}(d) = 2\lambda_c \pi d e^{-\lambda_c \pi d^2}. \tag{46}$$

After taking the average over  $L(\|x_1\|)$ , the expression in Proposition 1 can be easily obtained.

## B. Proof for Proposition 2

To successfully decode CoMP user's message, the following two conditions must be met.

- 1) The NOMA user's message can be successfully decoded, i.e.,  $\text{SINR}_{k_1^*}^{\text{BS}_1} > \epsilon_1$

2) After removing the NOMA user's message, the CoMP user's message can be decoded,

$$\text{i.e., } \frac{\phi |h_{\text{BS}_1, \text{U}_0}|^2}{I_{\text{inter}}^U + \frac{1}{\rho}} > \epsilon_0.$$

As such, the outage probability of the CoMP user can be expressed as

$$P_0^{\text{nearest}} = \mathcal{E}_{d, I_{\text{inter}}^U} \{P_0^{\text{nearest}}(d, I_{\text{inter}}^U)\}, \quad (47)$$

where  $P_0^{\text{nearest}}(d, I_{\text{inter}}^U)$  is the outage probability given a fixed  $d$  and  $I_{\text{inter}}^U$ , and can be calculated as follows:

$$\begin{aligned} P_0^{\text{nearest}}(d, I_{\text{inter}}^U) &= 1 - \int_{\frac{\epsilon_0 d^4 (I_{\text{inter}}^U + 1/\rho)}{\phi}}^{\infty} \int_{\epsilon_1 (\frac{\phi x}{d^4} + I_{\text{inter}}^U + \frac{1}{\rho})}^{\infty} f_{|h_{\text{BS}_1, \text{U}_0}|^2}(x) f_{z_{k_1^*, 1}}(y) dx dy \quad (48) \\ &= 1 + \sum_{\substack{k_0 + \dots + k_N = K \\ k_0 \neq K}} \binom{K}{k_0, \dots, k_N} \prod_{n=0, k_n \neq 0}^N \tilde{w}_n^{k_n} e^{-k_n \tilde{c}_n \epsilon_1 \frac{1}{\rho}} \\ &\quad \times \exp\left(-\left(\epsilon_1 \mu + \frac{\epsilon_0 (\phi \epsilon_1 \mu + d^4)}{\phi}\right) I_{\text{inter}}^U\right) \\ &\quad \times \frac{d^4}{\phi \epsilon_1 \mu + d^4} \exp\left(-\frac{\epsilon_0 (\phi \epsilon_1 \mu + d^4)}{\phi \rho}\right). \end{aligned}$$

By applying the Laplace transform of  $I_{\text{inter}}^U$  as expressed in (42) and taking the average over  $d$ , the expression in (26) is obtained and the proof for Proposition 2 is complete.

## REFERENCES

- [1] Y. Saito, Y. Kishiyama, A. Benjebbour, T. Nakamura, A. Li, and K. Higuchi, "Non-orthogonal multiple access (NOMA) for cellular future radio access," in *Proc. IEEE Veh. Technol. Conf.*, Dresden, Germany, Jun. 2013, pp. 1–5.
- [2] Z. Ding, X. Lai, G. K. Karagiannidis, R. Schober, J. Yuan, and V. Bhargava, "A survey on non-orthogonal multiple access for 5G networks: research challenges and future trends," *IEEE J. Sel. Areas Commun.*, vol. 35, no. 10, pp. 2181–2195, Oct. 2017.
- [3] Z. Ding, Y. Liu, J. Choi, Q. Sun, M. Elkashlan, I. Chih-Lin, and H. V. Poor, "Application of non-orthogonal multiple access in LTE and 5G networks," *IEEE Commun. Mag.*, vol. 55, no. 2, pp. 185–191, Feb. 2017.
- [4] S. R. Islam, N. Avazov, O. A. Dobre, and K.-S. Kwak, "Power-domain non-orthogonal multiple access (NOMA) in 5G systems: Potentials and challenges," *IEEE Commun. Surveys Tuts.*, vol. 19, no. 2, pp. 721–742, Sec. 2017.
- [5] *Study on Downlink Multiuser Superposition Transmission for LTE*, 3rd Generation Partnership Project, Mar. 2015.
- [6] L. Zhang et al., "Layered-division-multiplexing: Theory and practice," *IEEE Trans. Broadcast.*, vol. 62, no. 1, pp. 216–232, Mar. 2016.
- [7] Z. Ding, Z. Yang, P. Fan, and H. V. Poor, "On the performance of non-orthogonal multiple access in 5G systems with randomly deployed users," *IEEE Signal Process. Lett.*, vol. 21, no. 12, pp. 1501–1505, Dec. 2014.
- [8] Z. Ding, M. Peng, and H. V. Poor, "Cooperative non-orthogonal multiple access in 5G systems," *IEEE Communications Letters*, vol. 19, no. 8, pp. 1462–1465, Aug. 2015.
- [9] S. Timotheou and I. Krikidis, "Fairness for non-orthogonal multiple access in 5G systems," *IEEE Signal Process. Lett.*, vol. 22, no. 10, pp. 1647–1651, Oct. 2015.

- [10] Z. Ding, P. Fan, and H. V. Poor, "Impact of user pairing on 5G nonorthogonal multiple-access downlink transmissions," *IEEE Trans. Veh. Technol.*, vol. 65, no. 8, pp. 6010–6023, Aug. 2016.
- [11] P. Xu and K. Cumanan, "Optimal power allocation scheme for non-orthogonal multiple access with  $\alpha$ -fairness," *IEEE J. Select. Areas Commun.*, vol. 35, no. 10, pp. 2357–2369, Oct. 2017.
- [12] S. R. Islam, M. Zeng, O. A. Dobre, and K.-S. Kwak, "Resource allocation for downlink NOMA systems: Key techniques and open issues," *IEEE Wireless Commun.*, vol. 25, no. 2, pp. 40–47, Apr. 2018.
- [13] M. Zeng, A. Yadav, O. A. Dobre, and H. V. Poor, "Energy-efficient power allocation for MIMO-NOMA with multiple users in a cluster," *IEEE Access*, vol. 6, pp. 5170–5181, Feb. 2018.
- [14] H. Tabassum, E. Hossain, and J. Hossain, "Modeling and analysis of uplink non-orthogonal multiple access (NOMA) in large-scale cellular networks using poisson cluster processes," *IEEE Trans. Commun.*, vol. 65, no. 8, pp. 3555–3570, Aug. 2017.
- [15] Z. Zhang, H. Sun, and R. Q. Hu, "Downlink and uplink non-orthogonal multiple access in a dense wireless network," *IEEE J. Sel. Areas Commun.*, vol. PP, no. 99, pp. 1–1, Jul. 2017.
- [16] H. Nikopour and H. Baligh, "Sparse code multiple access," in *Proc. IEEE Int. Symposium on Personal Indoor and Mobile Radio Commun.*, London, UK, 2013, pp. 332–336.
- [17] X. Dai, S. Chen, S. Sun, S. Kang, Y. Wang, Z. Shen, and J. Xu, "Successive interference cancelation amenable multiple access (SAMA) for future wireless communications," in *Proc. IEEE Int. Conf. Commun. Systems*, Coimbatore, India, 2014, pp. 222–226.
- [18] Z. Ding, P. Fan, and H. V. Poor, "Random beamforming in millimeter-wave NOMA networks," *IEEE Access*, vol. 5, pp. 7667–7681, Feb. 2017.
- [19] Z. Ding, L. Dai, R. Schober, and H. V. Poor, "NOMA meets finite resolution analog beamforming in massive MIMO and millimeter-wave networks," *IEEE Commun. Lett.*, vol. PP, no. 99, pp. 1–1, Aug. 2017.
- [20] Z. Ding, R. Schober, and H. V. Poor, "A general MIMO framework for NOMA downlink and uplink transmission based on signal alignment," *IEEE Trans. Wireless Commun.*, vol. 15, no. 6, pp. 4438–4454, Jun. 2016.
- [21] M. Zeng, A. Yadav, O. A. Dobre, G. I. Tsiropoulos, and H. V. Poor, "Capacity comparison between MIMO-NOMA and MIMO-OMA with multiple users in a cluster," *IEEE J. Select. Areas Commun.*, vol. 35, no. 10, pp. 2413–2424, Oct. 2017.
- [22] J. Choi, "Minimum power multicast beamforming with superposition coding for multiresolution broadcast and application to NOMA systems," *IEEE Trans. Commun.*, vol. 63, no. 3, pp. 791–800, Mar. 2015.
- [23] M. Zeng, A. Yadav, O. A. Dobre, G. I. Tsiropoulos, and H. V. Poor, "On the sum rate of MIMO-NOMA and MIMO-OMA systems," *IEEE Wireless Commun. Lett.*, vol. 6, no. 4, pp. 534–537, Aug. 2017.
- [24] Z. Yang, Z. Ding, Y. Wu, and P. Fan, "Novel relay selection strategies for cooperative NOMA," *IEEE Trans. Veh. Technol.*, vol. 66, no. 11, pp. 10 114–10 123, Nov. 2017.
- [25] Z. Ding, P. Fan, G. K. Karagiannidis, R. Schober, and H. V. Poor, "NOMA assisted wireless caching: strategies and performance analysis," *IEEE Trans. Commun.*, to be published.
- [26] V. Jungnickel, L. Thiele, T. Wirth, T. Haustein, S. Schiffermuller, A. Forck, S. Wahls, S. Jaeckel, S. Schubert, H. Gabler *et al.*, "Coordinated multipoint trials in the downlink," in *Proc. IEEE Globecom. Workshops*, Honolulu, HI, USA, Dec. 2009, pp. 1–7.
- [27] M. Sawahashi, Y. Kishiyama, A. Morimoto, D. Nishikawa, and M. Tanno, "Coordinated multipoint transmission/reception techniques for LTE-advanced [Coordinated and Distributed MIMO]," *IEEE Wireless Commun.*, vol. 17, no. 3, Jun. 2010.
- [28] R. Irmer, H. Droste, P. Marsch, M. Grieger, G. Fettweis, S. Brueck, H.-P. Mayer, L. Thiele, and V. Jungnickel, "Coordinated multipoint: Concepts, performance, and field trial results," *IEEE Commun. Mag.*, vol. 49, no. 2, pp. 102–111, Feb. 2011.

- [29] L. Venturino, N. Prasad, and X. Wang, "Coordinated linear beamforming in downlink multi-cell wireless networks," *IEEE Trans. Wireless Commun.*, vol. 9, no. 4, pp. 1451–1461, Apr. 2010.
- [30] H. Dahrouj and W. Yu, "Coordinated beamforming for the multicell multi-antenna wireless system," *IEEE Trans. Wireless Commun.*, vol. 9, no. 5, pp. 1748–1759, May 2010.
- [31] J. Choi, "Non-orthogonal multiple access in downlink coordinated two-point systems," *IEEE Commun. Lett.*, vol. 18, no. 2, pp. 313–316, Feb. 2014.
- [32] Y. Sun, Z. Ding, X. Dai, and G. K. Karagiannidis, "A feasibility study on network NOMA," *IEEE Trans. Commun.*, to be published.
- [33] M. Haenggi, *Stochastic Geometry for Wireless Networks*. Cambridge, U.K.: Cambridge Univ. Press, 2012.
- [34] Y. J. Chun, M. O. Hasna, and A. Ghayeb, "Modeling heterogeneous cellular networks interference using poisson cluster processes," *IEEE J. Select. Areas Commun.*, vol. 33, no. 10, pp. 2182–2195, Oct. 2015.
- [35] H. David and H. Nagaraja, *Order Statistics*. 3rd, 3rd ed. Wiley, New York, NY, 2003.
- [36] W. Sun and J. Liu, "A Stochastic Geometry Analysis of CoMP-Based Uplink in Ultra-Dense Cellular Networks," in *Proc. IEEE Int. Conf. Commun. (ICC)*, May 2018, pp. 1–6.
- [37] —, "Coordinated multipoint based uplink transmission in Internet of Things powered by energy harvesting," *IEEE Internet of Things Journal*, vol. 5, no. 4, pp. 2585 – 2595, Dec. 2017.
- [38] H. Tabassum, Z. Dawy, E. Hossain, and M.-S. Alouini, "Interference statistics and capacity analysis for uplink transmission in two-tier small cell networks: A geometric probability approach," *IEEE Trans. Wireless Commun.*, vol. 13, no. 7, pp. 3837–3852, Jul. 2014.